Original Article

MOLECULAR METABOLISM

Fibroblast activation protein is dispensable for control of glucose homeostasis and body weight in mice

Brandon L. Panaro [1], Andrew L. Coppage [2], Jacqueline L. Beaudry [1], Elodie M. Varin [1], Kirandeep Kaur [1], Jack H. Lai [2], Wengen Wu [2], Yuxin Liu [2], William W. Bachovchin [2], Daniel J. Drucker [1,*]

ABSTRACT

Objective: Fibroblast Activation Protein (FAP), an enzyme structurally related to dipeptidyl peptidase-4 (DPP-4), has garnered interest as a potential metabolic drug target due to its ability to cleave and inactivate FGF-21 as well as other peptide substrates. Here we investigated the metabolic importance of FAP for control of body weight and glucose homeostasis in regular chow-fed and high fat diet-fed mice.

Methods: FAP enzyme activity was transiently attenuated using a highly-specific inhibitor CPD60 and permanently ablated by genetic inactivation of the mouse *Fap* gene. We also assessed the FAP-dependence of CPD60 and talabostat (Val-boroPro), a chemical inhibitor reportedly targeting both FAP and dipeptidyl peptidase-4

Results: CPD60 robustly inhibited plasma FAP activity with no effect on DPP-4 activity. *Fap* gene disruption was confirmed by assessment of genomic DNA, and loss of FAP enzyme activity in plasma and tissues. CPD60 did not improve lipid tolerance but modestly improved acute oral and intraperitoneal glucose tolerance in a FAP-dependent manner. Genetic inactivation of *Fap* did not improve glucose or lipid tolerance nor confer resistance to weight gain in male or female $Fap^{-/-}$ mice fed regular chow or high-fat diets. Moreover, talabostat markedly improved glucose homeostasis in a FAP- and FGF-21-independent, DPP-4 dependent manner.

Conclusion: Although pharmacological FAP inhibition improves glucose tolerance, the absence of a metabolic phenotype in $Fap^{-/-}$ *mice* suggest that endogenous FAP is dispensable for the regulation of murine glucose homeostasis and body weight. These findings highlight the importance of characterizing the specificity and actions of FAP inhibitors in different species and raise important questions about the feasibility of mouse models for targeting FAP as a treatment for diabetes and related metabolic disorders.

Keywords Diabetes; Obesity; Glucose; Body weight; Enzyme; Metabolism

1. INTRODUCTION

The metabolic roles of peptide hormones with endocrine activity have received considerable attention in the context of the rising incidence of diabetes and obesity. Notably, multiple gut hormones secreted from enteroendocrine cells control islet function and glucose homeostasis, and a subset of these hormones also regulate food intake, body weight, and lipid metabolism [1,2]. Furthermore, some members of the circulating fibroblast growth factor family, exemplified by fibroblast growth factor 21 (FGF-21), also exhibit hormone-like activity, and have been evaluated as therapeutic candidates for the treatment of diabetes, obesity, and non-alcoholic steatohepatitis [3,4]. The favorable metabolic actions of several gut hormones, notably glucose-dependent insulinotropic polypeptide (GIP) and glucagon-like-peptide-1 (GLP-1), have received considerable attention, and GLP-1 receptor agonists have been developed for the therapy of type 2 diabetes (T2D) and obesity [5].

A conserved feature shared by many peptide hormones is their short biological half-life, reflecting extraction and degradation by peripheral organs, urinary clearance, as well as enzymatic inactivation. Notably, N-terminal peptide cleavage by dipeptidyl peptidase-4 (DPP-4), the most extensively studied member of the DPP-4 activity and/or structure homologue (DASH) proteins [6], plays a critical role in terminating hormone action [7]. DPP-4 cleaves and inactivates GLP-1, oxyntomodulin, pituitary adenylate cyclase-activating peptide (PACAP), and glucose-dependent insulinotropic polypeptide (GIP), highlighting its key role in control of glucose homeostasis [8]. The biological importance of DPP-4 for control of islet function and glucose homeostasis has been demonstrated using mouse genetics, as well as through analysis of the biological activity of highly selective DPP-4 inhibitors in animals and humans [7,9,10]. Notably, genetic elimination of *Dpp4* in mice improves glucose homeostasis via potentiation of gut hormone action [11,12], findings mirrored by administration of small molecule highly selective DPP-4 inhibitors [7,9,10].

[1]Lunenfeld-Tanenbaum Research Institute, Sinai Health System, Toronto, ON M5G 1X5, Canada [2]Sackler School of Biomedical Sciences, Tufts University School of Medicine, Boston, MA, 02111, USA

*Corresponding author. Mt. Sinai Hospital 600 University Ave TCP5-1004, Toronto, ON M5G 1X5, Canada. Fax: +1 416 361 2669. E-mail: drucker@lunenfeld.ca (D.J. Drucker).

Received October 12, 2018 • Revision received October 30, 2018 • Accepted October 30, 2018 • Available online xxx

https://doi.org/10.1016/j.molmet.2018.10.011

Original Article

The therapeutic success of DPP-4 inhibitors for the treatment of T2D has stimulated interest in the metabolic actions of structurally-related DASH enzymes [6,7], including fibroblast activation protein (FAP)/seprase, a member of the DASH family with over 50% amino acid sequence identity with DPP-4 [13]. Intriguingly, both DPP-4 and FAP were first studied as candidate regulators of tumor cell growth, with elevated FAP expression detected within activated stromal fibroblasts of human epithelial cancers [14]. Both DPP-4 and FAP exhibit overlapping dipeptidyl peptidase activity and cleave a subset of similar substrates *ex vivo* [15]. In contrast to DPP-4, FAP also has a unique endopeptidase activity with a Gly—Pro specificity [16,17]. Furthermore, both DPP-4 and FAP exert activity as cell-anchored enzymes and via circulating soluble forms that retain enzyme activity [18,19]. FAP enzymatic activity is detectable, albeit at relatively low levels, in metabolically active tissues such as muscle, pancreas, and adipose tissue [19—21].

The observation that talabostat improves glucose homeostasis in mice was linked to FAP inhibition and potentiation of fibroblast growth factor-21 (FGF-21) activity [22]. However, early on, talabostat had been shown to be a potent DPP4 inhibitor [23] with glucose-lowering activity [24,25]. In fact, talabostat is ~20,000-fold more potent as an inhibitor of DPP-4 (Ki ~ 5 pM) than of FAP (Ki ~ 100 nM) [26]. Hence, ascribing anti-diabetic activities of talabostat to the inhibition of FAP can only be done in the absence of or concomitant inhibition of DPP-4 activity.

The emerging metabolic importance of FAP, and its overlapping structural and functional relationship to DPP-4, prompted us to further assess the importance of endogenous FAP in the control of glucose and lipid homeostasis. We therefore examined the effects of a potent and specific FAP inhibitor, (S)-N-(2-(2-Cyano-4,4-difluoropyrrolidin-1-yl)-2-oxoethyl)-quinoline-4-carboxamide [27] herein referred to as Compound 60 (CPD60), and found that it does indeed improve glucose tolerance, albeit modestly. In contrast, *Fap*$^{-/-}$ mice did not exhibit improved glucose control, or resistance to weight gain after prolonged high fat feeding. Furthermore, talabostat's anti-diabetic activities were independent of FGF21 or FAP. Taken together, our findings indicate that murine FAP is not a critical determinant of islet function, glucose homeostasis, weight gain, and the metabolic response to high fat feeding in mice.

2. MATERIALS AND METHODS

2.1. Animals

All animal studies were carried out according to protocols approved by Sinai Health System and The Centre for Phenogenomics (TCP, Toronto, Ontario, Canada). For studies using C57BL/6J mice, male animals aged 12 weeks or older were obtained from the in-house breeding colony at TCP. All mice were housed under specific pathogen-free conditions in ventilated microisolator cages and maintained on a 12-h light/dark cycle with free access to food and water unless otherwise noted. To account for sexual dimorphism, both males and females were studied in parallel for most experiments.

2.1.1. *Fap*$^{-/-}$ mice

Fap$^{-/-}$ (*Fap*^{em1Tcp}/Ddr) mice on a C57BL/6J background were generated at TCP by embryonic pronuclear microinjection of Cas9 mRNA and a single guide RNA with a spacer sequence of CCACTAAAGCAAGCGCAGCC, which resulted in a 5 bp deletion (GCGCT) in exon 2 at approximate position 62,573,481 bp (GRCm38) (confirmed by Sanger sequencing). This mutation is predicted to cause amino acid sequence changes after residue 15 and early truncation 17 amino acids later. Genotyping was performed using the following primers: Primer Fap-F (5′→3′): TCAAAAGCTCTGTGGGGAA; Primer Fap-R (5′→3′): GGTTTGGAATAATAGGGGCATAG. These primers amplify a 931 bp product, which, following digestion with Mwo1 (N.E.B. product #R0573S), yields a 794bp DNA fragment. In contrast, Mwo1 does not cleave a PCR product generated from homozygous knockout mouse DNA (see Figure S1).

2.1.2. *Fgf21*$^{-/-}$ mice

Fgf21$^{-/-}$ (Fgf21$^{tm1.1Djm}$; MGI:4354163) mice were re-derived at TCP after being obtained from the laboratory of Steven A. Kliewer and originally developed by David J. Mangelsdorf [28]. Genotyping was performed using the following primers: Primer F21SeqF1 (5′→3′): CCTCCAGATTTAGGAGTGCAGA; Primer F21GREV6-1 (5′→3′): GAAGACAGCCAGCAGCAGTCG; Primer F21NeoRev3 (5′→3′): GCATCGCCTTCTATCGCCTTCTTG. Together, these primers amplify a 500bp band from DNA corresponding to a WT allele, and a 300bp band from DNA corresponding to a *Fgf21* mutant allele.

2.1.3. *Dpp4*$^{-/-}$ mice

Dpp4$^{-/-}$ (CD26$^{-/-}$) mice were maintained in the Drucker lab and genotyped as described [11,29].

2.2. Glucose, insulin, and lipid tolerance tests

All tests were performed following a 5-hour daytime fast to minimize stress, with blood samples collected via tail-vein. For oral or intraperitoneal glucose tolerance tests (OGTT and IPGTT, respectively), 1.5 g/kg of glucose was given at Time 0. Insulin Tolerance Tests (ITT) were performed using a single IP dose of 0.7U/kg insulin (Humulin R, Eli Lilly) for lean RC-fed mice, or 1.2U/kg for HFD-fed mice. For Lipid Tolerance Tests (LTT), a 200 μL gavage of olive oil (Sigma) was administered and blood samples were collected for up to 180 min and assayed for non-esterified fatty acids (NEFAs) using NEFA-HR(2) (Wako) or triglycerides (TGs) using the Trig-GB kit (Roche). Blood samples were collected in K3-EDTA coated Microvette tubes (Sarstedt) (volume 50—100 μl) and, when measuring hormones at the indicated time points, mixed with 5—10 μl of a chilled solution containing 5000 kIU/ml Trasylol (Bayer), 32 mM EDTA, and 0.01 mM Diprotin A (Sigma) to prevent degradation. When applicable, drug pre-treatment using CPD60 or talabostat (Val-boroPro), acquired from the laboratory of Dr. William Bachovchin (Tufts University, Boston MA, USA) was performed by oral gavage 30—40 min prior to glucose treatments.

2.3. Hormone and enzymatic assays

Plasma insulin levels were measured in 5 μL volumes using the Ultrasensitive Mouse Insulin ELISA (Alpco Diagnostics). Plasma glucagon was measured using a 10 μL Glucagon ELISA (Mercodia). Fasting FGF-21 was measured from a single tail-vein bleed following an 18 h fast using the Rat/Mouse FGF 21 ELISA Kit (Millipore). For analysis of FAP activity, 3144-AMC was used as a FAP-specific fluorogenic substrate [19] (obtained from Dr. William Bachovchin, Tufts University), along with a reference AMC curve ranging from 0 to 50 μM. A 1:60 dilution of plasma in PBS was combined with 50uM 3144-AMC, shaken, and incubated at 37 °C with measurements (Ex. 360mn/Em. 460 nm) taken every 5 min over a 1 h time course in a temperature controlled EnSpire 2300 multilabel plate reader (PerkinElmer). For tissue FAP activity assays, ~80—120 mg of each tissue was homogenized using TissueLyser II with stainless steel bead agitation in a buffer containing 1 mM EDTA, 10% w/v glycerol, 0.02% Brij-35, 50 mM Tris—HCl, pH 8. The resulting homogenate was diluted 1:10 in PBS and assayed as

MOLECULAR METABOLISM

above. This protocol was adapted from [19]. For plasma DPP-4 activity, H-Gly-Pro-AMC HBr (Bachem #I-1225) was used as a substrate and plasma samples assayed in a 20-minute room-temperature timed protocol as described previously [30]. A single dose of CPD60 (20 mg/kg) produced sustained (more than 75%) inhibition of FAP activity for at least 12 h (Figure 1A and unpublished observations).

2.4. Magnetic resonance imaging (MRI), indirect calorimetry, and locomotor activity

For assessment of body composition, a whole body magnetic resonance analyzer was used (EchoMRI-100, Echo Medical Systems). Measures of O_2 consumption, CO_2 production, respiratory quotient, heat production, and physical activity were obtained after 2 days of acclimatization and 1 day of measurement using a Rodent Oxymax system (Columbus Instruments). Food intake was obtained manually by weighing food before and after 3 days in metabolic cages.

2.5. Gene expression analysis

RNA was isolated from various tissues according to the manufacturer's protocol (Tri-Reagent, Molecular Research Center Inc., Cincinnati, OH). Homogenization was performed in a medium-throughput manner using the TissueLyser II (Quiagen) with stainless steel beads. First-strand cDNA was synthesized using SuperScript III reverse transcriptase (Invitrogen) and random hexamers. Quantitative polymerase chain reaction (qPCR) was performed using the QuantStudio 5 Real-Time PCR System (ThermoFisher) and TaqMan Gene Expression Assays and Universal PCR Master Mix (Applied Biosystems) using the following TaqMan primers: *Fap* (Mm01329177_m1), *Dpp4* (Mm00494538_m1), *Dpp8* (Mm01151441_m1), *Dpp9* (Mm00841122_m1), *Fgf21* (Mm00840165_g1).

2.6. Histological analysis

Following animal sacrifice, liver and pancreata were isolated and then formalin-fixed and paraffin embedded, sliced at 4 μm thickness, and slide-mounted. H&E staining of livers and immunostaining of insulin and glucagon in pancreata, as well as slide scanning (ScanScopeCS System, Aperio Technologies) was performed by the Pathology Services facility at the Lunenfeld-Tanenbaum Research Institute. Quantification of α-cell and β-cell area was performed using positive pixel count analysis on Aperio ImageScope Viewer software (Leica Biosystems), with weak positive pixels discounted to minimize the effects of non-specific staining.

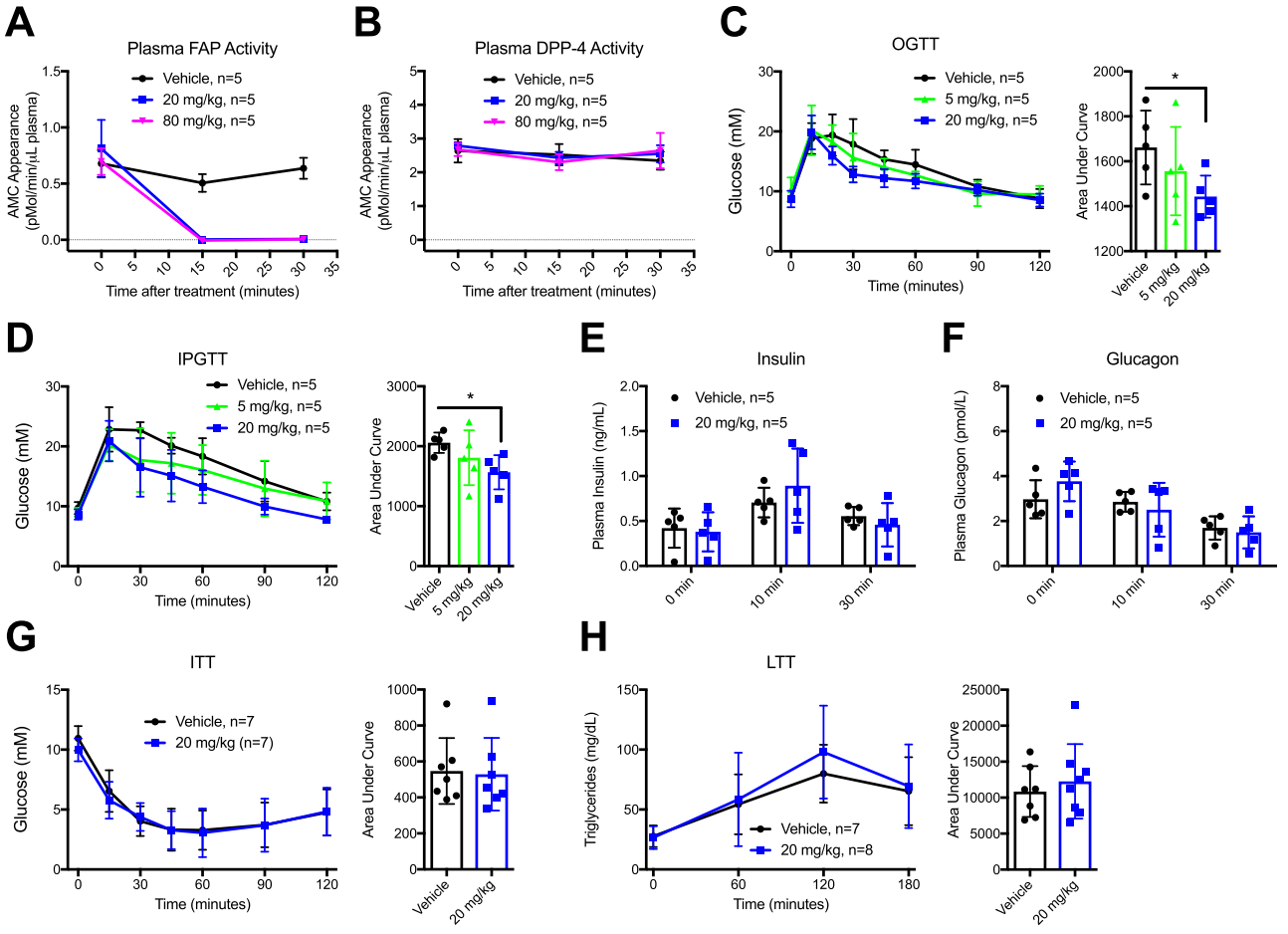

Figure 1: Pharmacological inhibition of FAP improves glucose homeostasis without affecting plasma levels of insulin or glucagon. CPD60 was given by oral gavage and FAP and DPP-4 activity were measured in 16-week old male C57BL/6J mice. Then, the mice were placed on a HFD for 2–3 weeks and given the indicated doses of either CPD60 or vehicle (PBS) by oral gavage 30 min prior to each test. **A)** Plasma FAP activity following CPD60 treatment. **B)** Plasma DPP-4 activity following CPD60 treatment. **C)** Oral glucose tolerance test (OGTT) at various doses of CPD60 and area under curve analysis (AUC) (right). **D)** Intraperitoneal Glucose Tolerance Test (IPGTT) and AUC. **E)** Insulin levels during OGTT. **F)** Glucagon levels during OGTT. **G)** Insulin Tolerance Test (ITT) and AUC. **H)** Triglycerides (TGs) and AUC during a Lipid Tolerance Test (LTT). Results were analyzed using ANOVA (Panels C and D), Two-way ANOVA (Panels E and F) or two-tailed *t*-test (Panels G and H). *P $<$ 0.05.

Original Article

2.7. Data analysis

All data were graphed and analyzed using GraphPad Prism, version 7.0d. Data are presented as mean +/− SD. Analyses performed included non-linear regression, ANOVA, 2-way ANOVA, two-tailed *t*-test, and paired *t*-test where appropriate. A *P* value less than 0.05 was considered to be statistically significant.

3. RESULTS

3.1. Pharmacological FAP inhibition improves glucose tolerance

To study the effects of acute FAP inhibition on glucose tolerance, we used a relatively selective FAP inhibitor *(S)-N-(2-(2-Cyano-4,4-difluoropyrrolidin*-1-yl*)-2-oxoethyl)- quinoline-4-carboxamide*, CPD60 [27,31], previously demonstrated to completely suppress FAP activity in mouse plasma [32]. When administered orally, CPD60 robustly inhibited plasma FAP enzymatic activity as early as 15 min post-gavage (Figure 1A). In contrast, the same doses of CPD60 had no effect on plasma DPP-4 activity (Figure 1B). Nevertheless, despite marked inhibition of FAP activity, CPD60 only modestly reduced glycemic excursion during oral and intraperitoneal glucose tolerance tests in a dose-dependent manner (Figure 1C—D), without concomitant changes in plasma levels of insulin and glucagon. Insulin sensitivity approximated by insulin tolerance testing was not different following administration of CPD60 (Figure 1E—G). Moreover, plasma triglycerides assessed following olive oil gavage were not different in the presence or absence of CPD60 (Figure 1H).

3.2. *Fap*$^{-/-}$ mice have reduced plasma and tissue FAP activity

To determine the importance of endogenous FAP activity for metabolic homeostasis independent of chemical enzyme inhibition, we used CRISPR/Cas9-mediated mutagenesis to generate *Fap*$^{-/-}$ mice on a C57BL/6J genetic background. A 5 base-pair deletion in exon 2 was predicted to produce a truncated non-functional FAP protein (Figure 2A). Indeed, we observed complete loss of plasma FAP activity in *Fap*$^{-/-}$ mice, with an intermediate reduction of plasma FAP activity in *Fap*$^{+/-}$ mice (Figure 2B, C). Furthermore, tissue FAP activity was markedly reduced or undetectable in pancreas, liver, muscle and adipose tissue of regular chow (RC)- or high fat diet (HFD)-fed *Fap*$^{-/-}$ mice (Figure 2D). Taken together, these findings substantiate the functional elimination of circulating and tissue FAP enzymatic activity in *Fap*$^{-/-}$ mice.

3.3. *Fap*$^{-/-}$ mice do not exhibit abnormalities in body weight or glucose homeostasis

FAP substrates include neuropeptides and metabolically active hormones such as FGF-21, known to regulate islet function, insulin sensitivity, and body weight [15,22]. Accordingly, we assessed

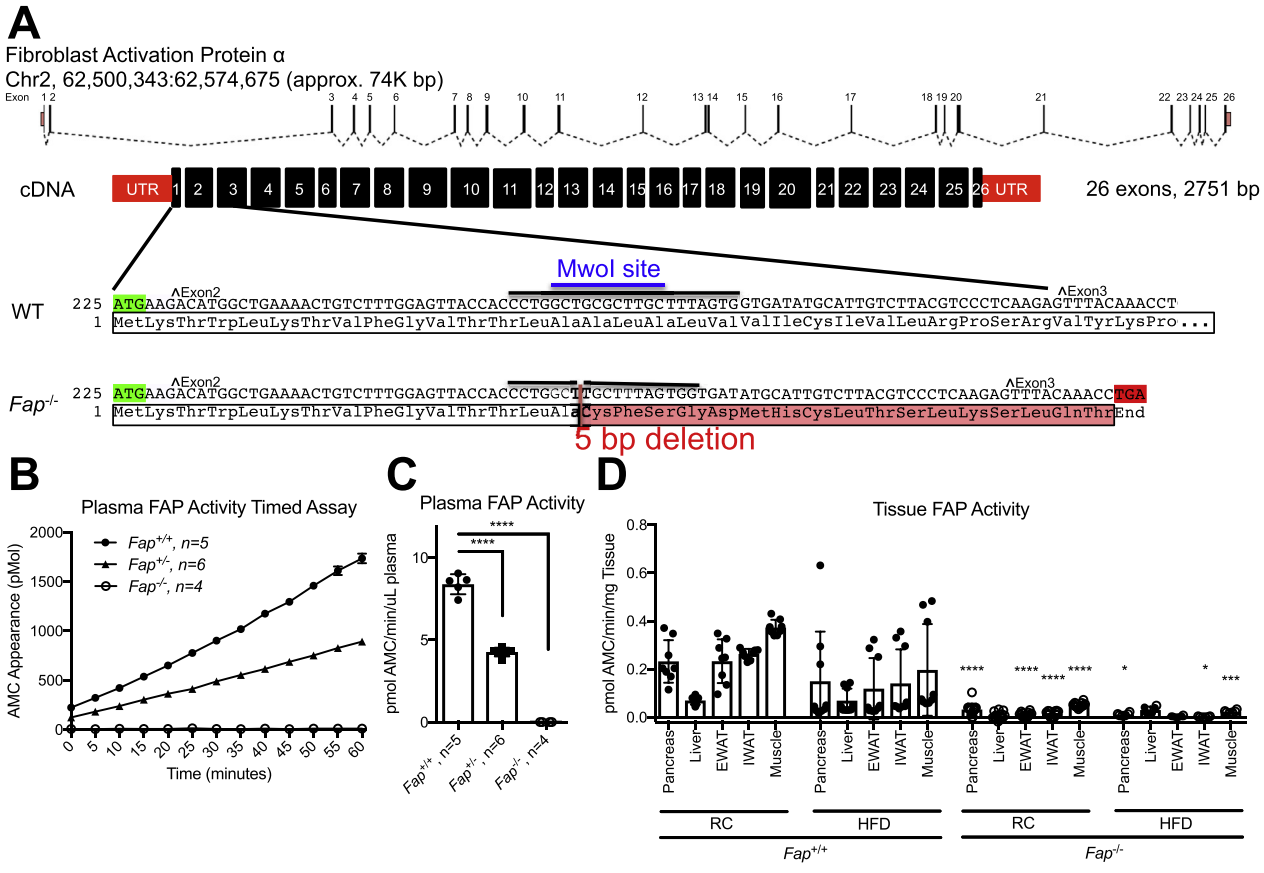

Figure 2: Generation and characterization of *Fap*$^{-/-}$ mice. A) A map of the FAP gene in mice and the partial cDNA sequence of wild-type and mutant *Fap* alleles are shown. The mutation causes a 5bp deletion and frame-shift occurring in exon 2 that is predicted to cause amino acid changes after Ala15 and an early truncation of the protein 17 amino acids later in exon 3. Start codon is in green; stop codons are in red. Black line indicates sequence targeted by guide RNA. ^ indicates a new exon. **B)** AMC appearance over time during FAP activity assay in *Fap*$^{+/+}$, $^{+/-}$, $^{-/-}$ mice. **C)** Average FAP activity (slope analysis) over duration of FAP activity assay. **D)** FAP activity in various tissues from *Fap*$^{+/+}$. Statistical significance was determined with ANOVA. *P < 0.05, ***P < 0.001, ****P < 0.0001, when compared to corresponding *Fap*$^{+/+}$ control groups.

MOLECULAR METABOLISM

metabolic homeostasis in RC-fed *Fap*$^{-/-}$ mice (Figure S2). Body weight and body composition were not different in male (Figure 3A—B) and female (Figure S3A,B) *Fap*$^{+/+}$ vs. *Fap*$^{-/-}$ mice; daily food intake was modestly reduced in male (Figure 3C) but not in female *Fap*$^{-/-}$ mice (Figure S3C). Moreover, male *Fap*$^{-/-}$ mice did not exhibit differences in oral or intraperitoneal glucose tolerance, insulin sensitivity, nor changes in corresponding levels of insulin or glucagon in the fasting state, or during glucose or insulin challenge (Figure 3D—L). Glucose tolerance and insulin sensitivity were also comparable in *Fap*$^{+/+}$ vs. *Fap*$^{-/-}$ female mice (Figure S3D—G). Furthermore, plasma triglyceride levels measured following olive oil gavage did not differ in *Fap*$^{+/+}$ vs. *Fap*$^{-/-}$ mice (Figure 3M). Metabolic parameters including VO_2, VCO_2, respiratory exchange ratio (RER), heat production, and locomotor activity were not different in male or female *Fap*$^{+/+}$ vs. *Fap*$^{-/-}$ (Figure S4). Hence, in the absence of a superimposed metabolic stress such as a high fat diet, germline loss of FAP is not associated with impaired regulation of glucose or energy homeostasis in RC-fed mice up to 40 weeks of age.

3.4. *Fap*$^{-/-}$ mice are not protected from obesity and hyperglycemia after high fat diet feeding

Given the lack of metabolic phenotypes in RC-fed *Fap*$^{-/-}$ mice, we studied male and female *Fap*$^{-/-}$ mice after several months of HFD feeding (Figure S2). No differences in body weight or body composition were detected after 22 wks of HFD feeding, although food intake was reduced in male, but not in female *Fap*$^{-/-}$ mice (Figure 4A—C, Figure S5A-C). Moreover, oral and intraperitoneal glucose tolerance, insulin sensitivity, and plasma levels of insulin and glucagon were not different either in the fasted state, or when assessed after glucose administration, in HFD-fed *Fap*$^{+/+}$ vs. *Fap*$^{-/-}$ mice (Figure 4D—L, Figure S5D-F). Similarly, plasma triglycerides were not different following olive oil gavage in *Fap*$^{+/+}$ vs. *Fap*$^{-/-}$ mice (Figure 4M, Figure S5G). Furthermore, respiratory rates, RER, and locomotor activity were similar in male and female *Fap*$^{+/+}$ vs. *Fap*$^{-/-}$ mice (Figure S6). Consistent with the observations of unchanged glucose tolerance and lipid tolerance, *Fap*$^{-/-}$ mice did not exhibit abnormalities of pancreatic histology, including β-cell and α-cell area, and liver morphology compared to *Fap*$^{+/+}$ controls (Figure S7). Taken together, these results demonstrate that whole body germline elimination of FAP does not impair glucose homeostasis, islet hormone responses, or the control of body weight and metabolism, in RC- or HFD-fed *Fap*$^{-/-}$ mice.

3.5. Relative expression of mRNA transcripts encoding related members of the DASH enzyme family

To assess whether the normal metabolic phenotype in *Fap*$^{-/-}$ mice might reflect compensatory upregulation of the expression of related DASH family genes, we examined mRNA levels of *Dpp4*, *Dpp8*, *Dpp9*, and the putative FAP substrate *Fgf21* in liver, epididymal white adipose tissue (eWAT), inguinal white adipose tissue (iWAT), pancreas, and muscle from *Fap*$^{+/+}$ and *Fap*$^{-/-}$ mice after RC or HFD feeding. No evidence for upregulation of these mRNA transcripts in *Fap*$^{-/-}$ mouse tissues was observed (Figure S8). Analysis of relative expression levels reported according to uncorrected CT values indicated the highest levels of *Fap* mRNA expression within muscle and adipose tissues (Figure S9).

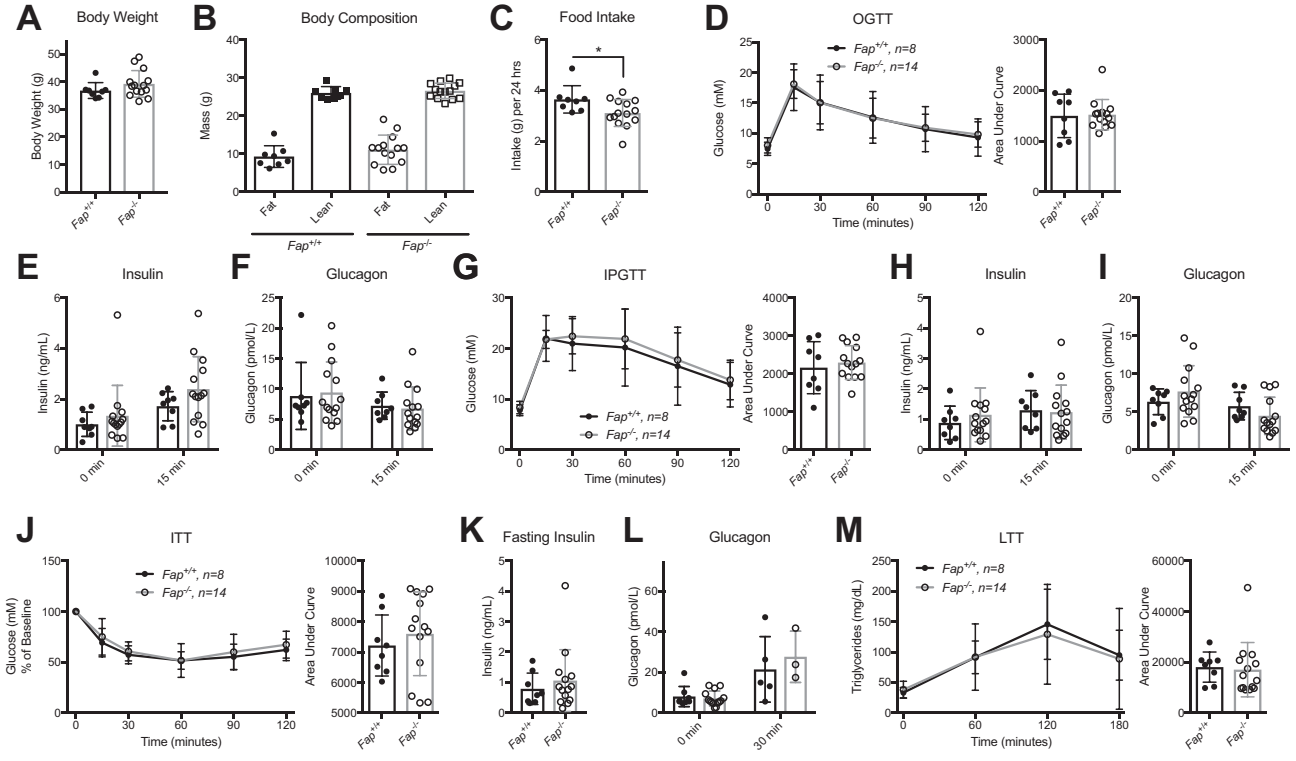

Figure 3: Male *Fap*$^{-/-}$ mice fed normal rodent chow exhibit normal body weight, glucose and lipid tolerance. Adult male *Fap*$^{+/+}$ and $^{-/-}$ mice were provided with RC and subjected to weekly metabolic tests beginning at 24 weeks of age. **A)** Body weight. **B)** Body composition. **C)** Average 24-hour food intake. **D)** OGTT and AUC analysis. **E)** Plasma insulin during OGTT. **F)** Plasma glucagon during OGTT. **G)** IPGTT and AUC analysis. **H)** Plasma insulin during IPGTT. **I)** Plasma glucagon during IPGTT. **J)** ITT and AUC analysis. **K)** Fasting plasma insulin prior to ITT. **L)** Plasma glucagon during ITT. **M)** TG levels during LTT and AUC analysis. Data were analyzed using 2-way ANOVA or two-tailed *t*-test. *P $<$ 0.05.

Original Article

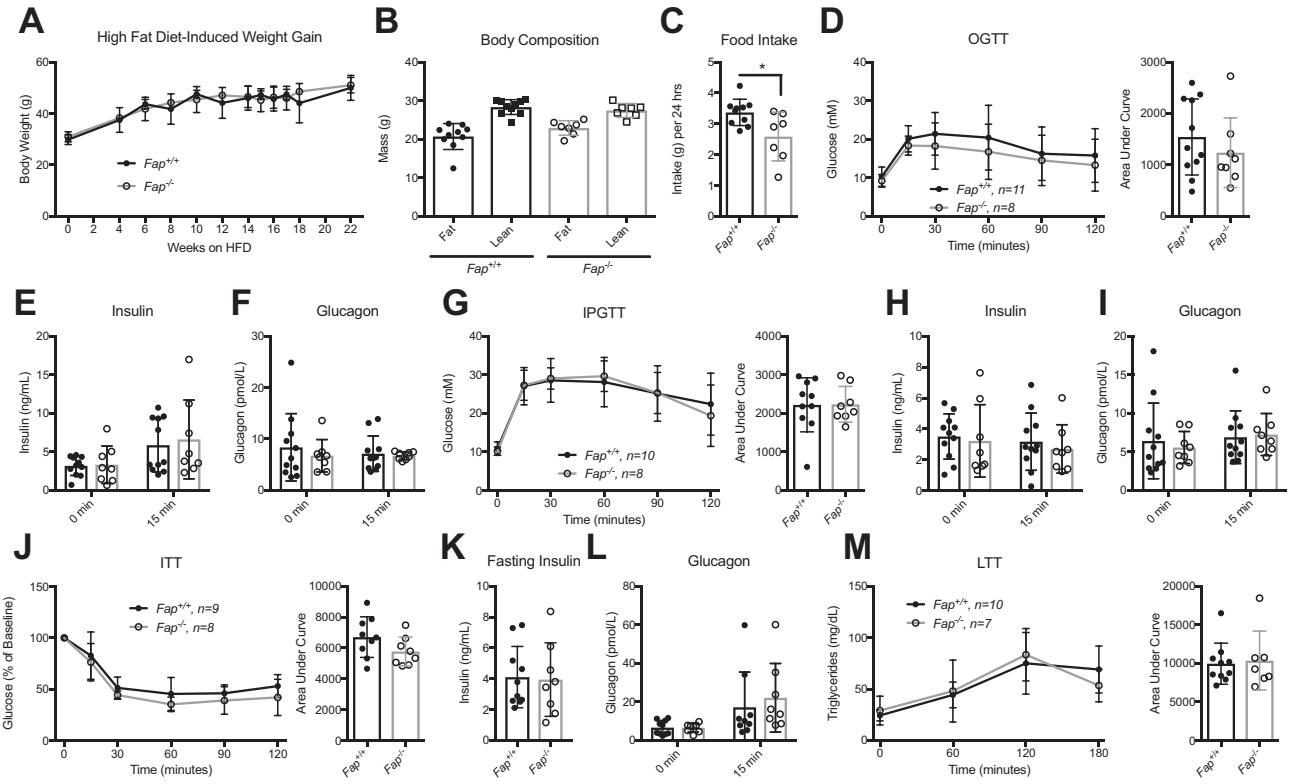

Figure 4: Male *Fap*$^{-/-}$ mice fed a HFD develop obesity and insulin resistance similar to control mice. Beginning at 12 weeks of age, male *Fap*$^{+/+}$ and $^{-/-}$ mice were given chronic ad libitum access to 45% kcal fat HFD. Tests were conducted weekly, starting at 24 weeks of age. **A)** HFD induced weight gain. **B)** Body composition. **C)** Food intake. **D)** OGTT and AUC analysis. **E)** Plasma insulin during OGTT. **F)** Plasma glucagon during OGTT. **G)** IPGTT and AUC analysis. **H)** Plasma insulin during IPGTT. **I)** Plasma glucagon during IPGTT. **J)** ITT and AUC analysis. **K)** Fasting plasma insulin prior to ITT. **L)** Plasma glucagon during ITT. **M)** TG levels during LTT and AUC analysis. Data were analyzed using 2-way ANOVA or two-tailed *t*-test. *P $<$ 0.05.

3.6. Pharmacological FAP inhibition does not lower glucose in *Fap*$^{-/-}$ mice

To reconcile the reduction of glucose excursion observed following acute inhibition of FAP activity using CPD60 with the normal glucose tolerance in *Fap*$^{-/-}$ mice, we used *Fap*$^{-/-}$ mice to assess the specificity of CPD60. Although glucose excursion was reduced in CPD60-treated *Fap*$^{+/+}$ mice during an OGTT, no glucose-lowering effect of CPD60 was detected in *Fap*$^{-/-}$ mice (Figure 5A, B) and plasma levels of insulin and glucagon were not different in *Fap*$^{+/+}$ vs. *Fap*$^{-/-}$ mice in the presence or absence of CPD60 (Figure 5C, D). Hence, CPD60 requires FAP to acutely improve oral glucose tolerance.

3.7. Talabostat inhibits DPP-4 enzymatic activity and requires *Dpp4* to improve glucose tolerance

The finding that complete genetic elimination of FAP activity produces no substantial metabolic phenotype contrasts with the metabolic benefits previously ascribed to pharmacological FAP inhibition with talabostat (Val-boroPro) [22]. Talabostat has been reported to potentiate FGF-21 activity, through actions ascribed to enzymatic FAP inhibition [22,33]; however, talabostat is first and foremost a DPP4 inhibitor and therefore also exerts anti-diabetic activity via inhibition of DPP-4 [23,25,26,34,35]. To reconcile these findings, we compared the acute actions of talabostat in *Fgf21*$^{-/-}$, *Dpp4*$^{-/-}$, and *Fap*$^{-/-}$ mice and their littermate controls. Notably, talabostat improved glucose tolerance and increased plasma insulin levels in *Fgf21*$^{-/-}$ mice (Figure 6A–C). In contrast, talabostat was highly effective at lowing glucose excursions in *Dpp4*$^{+/+}$ but not in *Dpp4*$^{-/-}$ mice (Figure 6D, E), without further augmentation of plasma insulin levels (Figure 6F). Interestingly, talabostat acutely improved glucose homeostasis in both *Fap*$^{+/+}$ and *Fap*$^{-/-}$ mice, without further augmentation of insulin levels (Figure 6G–I). Consistent with these findings, talabostat potently inhibited plasma DPP-4 activity in all groups and had little effect on FAP activity at the dose used; in contrast CPD60 suppressed FAP, but not DPP-4 activity (Figure 6J–K). Furthermore, no genotype or drug-dependent changes in total immunoreactive FGF-21 levels were detected in the fasted state (Figure 6L). Taken together, these results indicate that germline genetic elimination of *Fap* in mice is not associated with improvements in glucose control or resistance to diet-induced obesity. Furthermore, the metabolic benefits ascribed to talabostat administration likely reflect actions predominantly arising from potent inhibition of DPP-4, and not FAP activity.

4. DISCUSSION

Our current experiments directed at elucidating the metabolic importance of FAP were motivated by recent studies supporting a role for FAP in control of glycemia and body weight [22], together with an extensive literature highlighting the metabolic importance of the structurally and functionally related DASH enzyme, DPP-4 [7,9,10]. Notably, plasma levels of both DPP-4 and FAP activity are increased in human subjects with T2D [36,37], consistent with the possibility that increased expression of one or both enzymes contributes to the development of dysglycemia via degradation of glucoregulatory substrates. Indeed, DPP-4 has been extensively validated, in studies

MOLECULAR METABOLISM

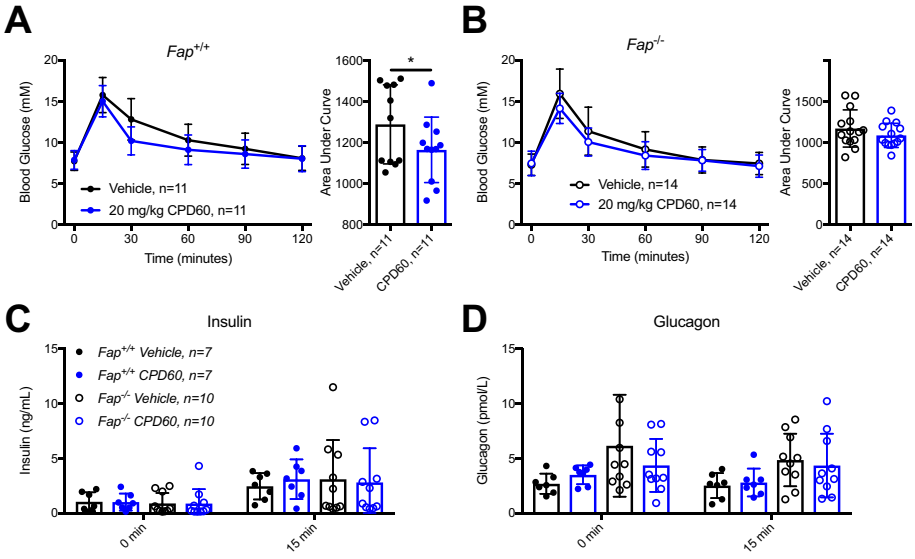

Figure 5: Pharmacological FAP inhibition does not lower glucose in *Fap*$^{-/-}$ mice. Adult *Fap*$^{+/+}$ and *Fap*$^{-/-}$ mice were treated with oral CPD60 or vehicle 30 min prior to each test in a 2 treatment crossover study. **A)** OGTT with vehicle or CPD60 in *Fap*$^{+/+}$ mice and AUC analysis. **B)** OGTT with vehicle or CPD60 in *Fap*$^{-/-}$ mice and AUC analysis. **C)** Insulin levels during OGTT. **D)** Glucagon levels during OGTT. 2-way ANOVA revealed no significant differences in hormone response to drug within genotypes. AUC analyses were tested using paired *t*-tests. *P $<$ 0.05.

ranging from mouse genetics to clinical trials using DPP-4 inhibitors, as an essential enzyme regulating glucose homeostasis and islet function [7,9–11].

Several previous studies linking inhibition of FAP activity to reduction of glucose and body weight in mice [22] employed talabostat, a non-selective FAP inhibitor, that also inhibits other members of the structurally related DASH enzyme family, especially DPP4 [34]. Intriguingly, the favorable metabolic activity of talabostat, including reduction of glucose and body weight, and augmentation of circulating levels of FGF-21, was reported to be predominantly evident in mice with diet-induced obesity, and markedly attenuated in lean euglycemic mice [22]. Here we demonstrate that acute reduction of FAP activity, using CPD60, a highly selective FAP inhibitor [27,32], was associated with a modest but significant improvement in oral and intraperitoneal glucose tolerance without affecting insulin or glucagon levels. In contrast, complete elimination of FAP activity in *Fap*$^{-/-}$ mice was not associated with changes in glucose tolerance, islet hormones, or insulin sensitivity, even under conditions of prolonged HFD-feeding. Hence, collectively, our data suggest that, in contrast to the favorable metabolic phenotype described for *Dpp4*$^{-/-}$ mice [11], genetic loss of *Fap* is not essential for control of metabolic homeostasis in mice.

One simple explanation for the favorable metabolic actions of talabostat in obese mice [22], vs. the modest actions of the relatively FAP-selective CPD60, is the potent inhibition of DPP-4 activity by talabostat [25]. Indeed, our current findings verify that talabostat at the dose previously utilized [22] robustly reduces DPP-4 activity and not FAP activity, and fails to further improve glucose tolerance in *Dpp4*$^{-/-}$ mice. Notably, DPP-4 and FAP are co-expressed on several cell types [38], and have been shown to cleave an overlapping set of regulatory peptides, including neuropeptide Y (NPY), peptide YY, B-type natriuretic peptide and substance P [15]. FAP and DPP-4 also physically interact to form a heteromeric complex that retains functional enzyme activity [38,39]. Hence, it seems reasonable to explore the therapeutic potential of dual enzyme inhibitors for the treatment of metabolic disease, given the close inter-dependent structural and functional overlapping interactions demonstrated for FAP and DPP-4.

Enthusiasm for the exploration of single or dual FAP inhibitors as a therapeutic approach for treatment of metabolic disorders stems in part from the role of FAP in the cleavage and inactivation of FGF-21. Indeed, genetic ablation, immunodepletion, or pharmacological inhibition of FAP activity, with inhibitors such as CPD60, markedly inhibits the cleavage of human FGF-21 [32,33]. Nevertheless, the importance and biological activity of N-terminally cleaved forms of FGF-21 and their relationship to relative levels of total circulating immunoreactive FGF-21 has not been extensively assessed in humans. Although mouse FAP is capable of cleaving human FGF-21 [33], the extent to which mouse FGF-21 is cleaved and inactivated by mouse FAP is less certain. Mouse FGF-21 contains a Glu—Pro dipeptide at position 170—171 in place of the human Gly—Pro FAP cleavage sequence, which renders mouse FGF-21 relatively resistant to FAP cleavage at this site in the protein [32,33]. We did not observe differences in plasma levels of total immunoreactive FGF-21, measured in the fasting state, nor in *Fgf21* mRNA in several tissues in RC- or HFD-fed *Fap*$^{-/-}$ vs. *Fap*$^{+/+}$ mice. Indeed endogenous plasma FGF-21 levels were previously reported to be similar in littermate control *Fap*$^{+/+}$ vs. *Fap*$^{-/-}$ mice [32]. Although we demonstrate here that talabostat retained its acute glucoregulatory activity in *Fgf21*$^{-/-}$ mice, a 7 day course of talabostat did not fully improve glucose tolerance, reduce body weight or adiposity in *Fgf21*$^{-/-}$ mice, relative to its corresponding efficacy in *Fgf21*$^{+/+}$ littermate controls [22]. Moreover, plasma levels of FGF-21 were reported to be similar in *Fap*$^{+/+}$ vs. *Fap*$^{-/-}$ mice [32]. Hence, the importance of murine FGF-21 for transducing the acute and chronic metabolic actions of single FAP or dual FAP/DPP-4 inhibitors requires further investigation.

Our studies of Fgf-21 expression did not reveal induction of *Fgf21* mRNA transcripts in liver, muscle, fat, or pancreas of 40 wk-old male mice after prolonged high fat feeding. In contrast, FGF-21 expression was induced in multiple tissues in high fat fed monkeys [40], in mice fed a ketogenic diet [41], and pancreatic [42] and hepatic [43] levels of

Original Article

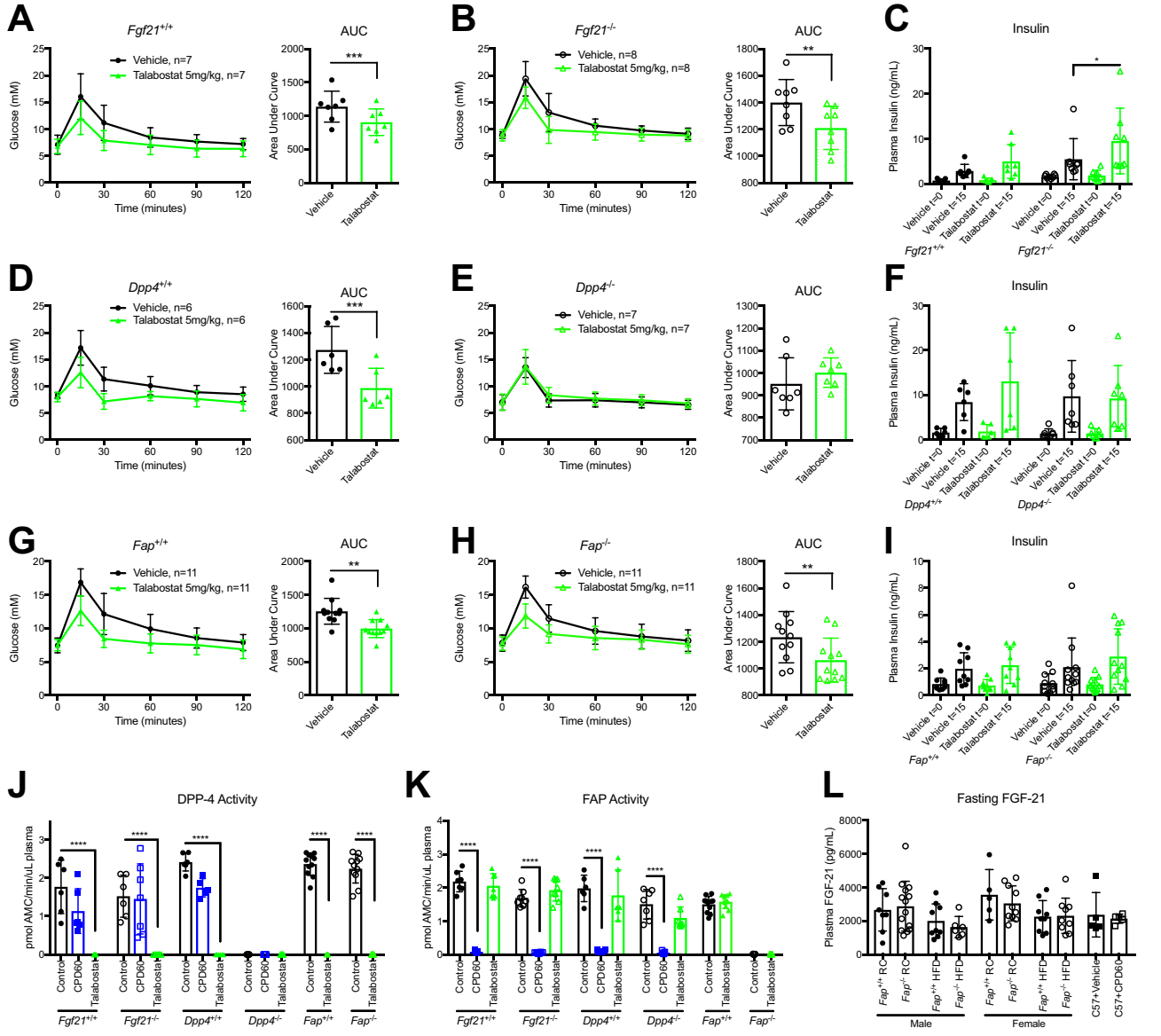

Figure 6: Talabostat lowers glucose independently of FAP and FGF-21. Adult *Fgf21*$^{+/+}$ and *Fgf21*$^{-/-}$, *Dpp4*$^{+/+}$ and *Dpp4*$^{-/-}$, and *Fap*$^{+/+}$ and *Fap*$^{-/-}$ mice were treated with either vehicle or talabostat (Val-boroPro) by oral gavage 30 min prior to an OGTT. **A, B)** 16-week old male *Fgf21*$^{+/+}$ and *Fgf21*$^{-/-}$ mice treated with talabostat prior to an OGTT, and AUC analyses. **C)** Insulin levels during OGTT in all treatment groups and *Fgf21* genotypes. **D, E)** 18-week old *Dpp4*$^{+/+}$ and *Dpp4*$^{-/-}$ mice treated with talabostat prior to an OGTT, and AUC analyses. **F)** Insulin levels during OGTT in all treatment groups and *Dpp4* genotypes. **G, H)** 30-week old male and female *Fap*$^{+/+}$ and *Fap*$^{-/-}$ mice treated with talabostat prior to an OGTT, and AUC analyses. **I)** Insulin levels during OGTT in all treatment groups and *Dpp4* genotypes. **J)** Plasma DPP-4 activity 45 min after treatment with CPD60 or talabostat in mice with different genotypes. **K)** Plasma FAP activity 45 min after CPD60 or talabostat administration. **L)** Plasma FGF-21 levels after an 18-hour fast in male and female *Fap*$^{+/+}$, *Fap*$^{-/-}$, and vehicle- or CPD60-treated C57BL6 mice. Due to the design of the crossover studies, data were analyzed using paired *t*-test. *P $<$ 0.05, **P $<$ 0.01, ***P $<$ 0.001, ****P $<$ 0.0001.

Fgf21 mRNA were upregulated in mice following high fat feeding. These differences in nutrient control of *Fgf21* expression may reflect species-specific differences and experimental conditions, including diets, genetic background, age, and sex of mice that differ in various studies across laboratories.

The generation and phenotypic characterization of *Fap*$^{-/-}$ mice has been described over 15 years ago, with reports of normal growth and development in the setting of complete absence of Fap protein and enzyme activity [44]. More recently, an independent line of *Fap*$^{-/-}$ mice generated on the C57BL/6 background for studies of cancer biology was reported to exhibit normal levels of plasma glucose, pancreatic weight, and pancreatic histology, although dynamic metabolic testing was not reported [45]. The findings reported here of normal glucose homeostasis and body weight in RC- and HFD-fed *Fap*$^{-/-}$ mice strongly suggest that FAP is not essential for the adaptive metabolic response to energy excess in mice.

5. CONCLUSIONS AND LIMITATIONS

Our studies in mice have several caveats, limiting extrapolation to human biology. First, the mouse FAP protein differs structurally and functionally from human FAP [19]. Although circulating FAP enzymatic

MOLECULAR METABOLISM

activity is relatively higher in mouse vs. human plasma [19], mouse FAP exhibited a lower catalytic activity, compared to human FAP, *ex vivo* [31]. Furthermore, it is possible that additional species-specific differences in the structure of putative metabolically active FAP substrates, beyond FGF-21, may further complicate interpretation of FAP biology in mice vs. humans. Notably, commercially available assays for measurement of FGF-21 in mice do not allow reliable discrimination of cleaved vs. intact forms of FGF-21, precluding definitive ascertainment of whether FAP cleaves FGF-21 in the studies reported here. Additionally, we studied mice with complete elimination of *Fap* in all tissues, and developmental adaptations and compensation in response to global germline elimination of FAP may modify the biological phenotypes arising from loss of FAP in one or more tissues. Notably, acute transient FAP inhibition with CPD60, a short-acting FAP inhibitor, does improve oral and intraperitoneal glucose tolerance via currently unknown mechanisms, hence a role for more sustained pharmacological FAP inhibition as a therapeutic opportunity for metabolic disorders such as diabetes cannot be excluded by our data. Taken together, these findings have relevance for the design of preclinical experimental paradigms to assess the therapeutic potential of FAP in the control of metabolism and energy homeostasis.

DISCLOSURES

The authors report no disclosures relevant to the study of mouse FAP biology.

ACKNOWLEDGMENTS

These studies were supported by a CIHR Foundation grant 154321 and a Banting and Best Diabetes Centre-Novo Nordisk Chair in Incretin Biology to DJD. BP was supported by a NIDDK Fellowship Award 5 F32 DK107050. JB and EV were supported by fellowship Awards from Diabetes Canada.

CONFLICT OF INTEREST

W. Bachovchin has filed patents, assigned to Tufts University, describing the development and characterization of FAP inhibitors. None of the other co-authors has any disclosures relevant to the current submission on FAP.

APPENDIX A. SUPPLEMENTARY DATA

Supplementary data to this article can be found online at https://doi.org/10.1016/j.molmet.2018.10.011.

REFERENCES

[1] Drucker, D.J., 2007. The role of gut hormones in glucose homeostasis. Journal of Clinical Investigation 117(1):24–32.

[2] Drucker, D.J., 2016. Evolving concepts and translational relevance of enteroendocrine cell biology. The Journal of Cinical Endocrinology and Metabolism 101(3):778–786.

[3] Fisher, F.M., Maratos-Flier, E., 2016. Understanding the physiology of FGF21. Annual Review of Physiology, 78223–78241.

[4] Staiger, H., Keuper, M., Berti, L., Hrabe de Angelis, M., Haring, H.U., 2017. Fibroblast growth factor 21-metabolic role in mice and men. Endocrine Reviews 38(5):468–488.

[5] Drucker, D.J., Habener, J.F., Holst, J.J., 2017. Discovery, characterization, and clinical development of the glucagon-like peptides. Journal of Clinical Investigation 127(12):4217–4227.

[6] Busek, P., Malik, R., Sedo, A., 2004. Dipeptidyl peptidase IV activity and/or structure homologues (DASH) and their substrates in cancer. The International Journal of Biochemistry & Cell Biology 36(3):408–421.

[7] Mulvihill, E.E., Drucker, D.J., 2014. Pharmacology, physiology and mechanisms of action of dipeptidyl peptidase-4 inhibitors. Endocrine Reviews(6):992–1019.

[8] Zhu, L., Tamvakopoulos, C., Xie, D., Dragovic, J., Shen, X., Fenyk-Melody, J.E., et al., 2003. The role of dipeptidyl peptidase IV in the cleavage of glucagon family peptides: in vivo metabolism of pituitary adenylate cyclase activating polypeptide-(1-38). Journal of Biological Chemistry 278(25):22418–22423.

[9] Ahren, B., Foley, J.E., 2016. Improved glucose regulation in type 2 diabetic patients with DPP-4 inhibitors: focus on alpha and beta cell function and lipid metabolism. Diabetologia 59(5):907–917.

[10] Deacon, C.F., 2018. Peptide degradation and the role of DPP-4 inhibitors in the treatment of type 2 diabetes. Peptides 100:150–157.

[11] Marguet, D., Baggio, L., Kobayashi, T., Bernard, A.M., Pierres, M., Nielsen, P.F., et al., 2000. Enhanced insulin secretion and improved glucose tolerance in mice lacking CD26. Proceedings of the National Academy of Sciences of the U S A 97(12):6874–6879.

[12] Conarello, S.L., Li, Z., Ronan, J., Roy, R.S., Zhu, L., Jiang, G., et al., 2003. Mice lacking dipeptidyl peptidase IV are protected against obesity and insulin resistance. Proceedings of the National Academy of Sciences of the U S A 100(11):6825–6830.

[13] Niedermeyer, J., Enenkel, B., Park, J.E., Lenter, M., Rettig, W.J., Damm, K., et al., 1998. Mouse fibroblast-activation protein–conserved Fap gene organization and biochemical function as a serine protease. European Journal of Biochemistry 254(3):650–654.

[14] Scanlan, M.J., Raj, B.K., Calvo, B., Garin-Chesa, P., Sanz-Moncasi, M.P., Healey, J.H., et al., 1994. Molecular cloning of fibroblast activation protein alpha, a member of the serine protease family selectively expressed in stromal fibroblasts of epithelial cancers. Proceedings of the National Academy of Sciences of the U S A 91(12):5657–5661.

[15] Keane, F.M., Nadvi, N.A., Yao, T.W., Gorrell, M.D., 2011. Neuropeptide Y, B-type natriuretic peptide, substance P and peptide YY are novel substrates of fibroblast activation protein-alpha. FEBS Journal 278(8):1316–1332.

[16] Aertgeerts, K., Levin, I., Shi, L., Snell, G.P., Jennings, A., Prasad, G.S., et al., 2005. Structural and kinetic analysis of the substrate specificity of human fibroblast activation protein alpha. Journal of Biological Chemistry 280(20):19441–19444.

[17] Edosada, C.Y., Quan, C., Tran, T., Pham, V., Wiesmann, C., Fairbrother, W., et al., 2006. Peptide substrate profiling defines fibroblast activation protein as an endopeptidase of strict Gly(2)-Pro(1)-cleaving specificity. FEBS Letters 580(6):1581–1586.

[18] Lee, K.N., Jackson, K.W., Christiansen, V.J., Lee, C.S., Chun, J.G., McKee, P.A., 2006. Antiplasmin-cleaving enzyme is a soluble form of fibroblast activation protein. Blood 107(4):1397–1404.

[19] Keane, F.M., Yao, T.W., Seelk, S., Gall, M.G., Chowdhury, S., Poplawski, S.E., et al., 2013. Quantitation of fibroblast activation protein (FAP)-specific protease activity in mouse, baboon and human fluids and organs. FEBS Open Bio 443:443–454.

[20] Roberts, E.W., Deonarine, A., Jones, J.O., Denton, A.E., Feig, C., Lyons, S.K., et al., 2013. Depletion of stromal cells expressing fibroblast activation protein-alpha from skeletal muscle and bone marrow results in cachexia and anemia. Journal of Experimental Medicine 210(6):1137–1151.

[21] Busek, P., Hrabal, P., Fric, P., Sedo, A., 2015. Co-expression of the homologous proteases fibroblast activation protein and dipeptidyl peptidase-IV in the adult human Langerhans islets. Histochemistry and Cell Biology 143(5):497–504.

[22] Sanchez-Garrido, M.A., Habegger, K.M., Clemmensen, C., Holleman, C., Muller, T.D., Perez-Tilve, D., et al., 2016. Fibroblast activation protein (FAP) as a novel metabolic target. Mol Metab 5(10):1015–1024.

[23] Coutts, S.J., Kelly, T.A., Snow, R.J., Kennedy, C.A., Barton, R.W., Adams, J., et al., 1996. Structure-activity relationships of boronic acid inhibitors of

dipeptidyl peptidase IV. 1. Variation of the P2 position of Xaa-boroPro dipeptides. Journal of Medicinal Chemistry 39(10):2087—2094.

[24] Connolly, B.A., Sanford, D.G., Chiluwal, A.K., Healey, S.E., Peters, D.E., Dimare, M.T., et al., 2008. Dipeptide boronic acid inhibitors of dipeptidyl peptidase IV: determinants of potency and in vivo efficacy and safety. Journal of Medicinal Chemistry 51(19):6005—6013.

[25] Poplawski, S.E., Lai, J.H., Sanford, D.G., Sudmeier, J.L., Wu, W., Bachovchin, W.W., 2011. Pro-soft Val-boroPro: a strategy for enhancing in vivo performance of boronic acid inhibitors of serine proteases. Journal of Medicinal Chemistry 54(7):2022—2028.

[26] Bachovchin, D.A., Koblan, L.W., Wu, W., Liu, Y., Li, Y., Zhao, P., et al., 2014. A high-throughput, multiplexed assay for superfamily-wide profiling of enzyme activity. Nature Chemical Biology 10(8):656—663.

[27] Jansen, K., Heirbaut, L., Verkerk, R., Cheng, J.D., Joossens, J., Cos, P., et al., 2014. Extended structure-activity relationship and pharmacokinetic investigation of (4-quinolinoyl)glycyl-2-cyanopyrrolidine inhibitors of fibroblast activation protein (FAP). Journal of Medicinal Chemistry 57(7):3053—3074.

[28] Potthoff, M.J., Inagaki, T., Satapati, S., Ding, X., He, T., Goetz, R., et al., 2009. FGF21 induces PGC-1alpha and regulates carbohydrate and fatty acid metabolism during the adaptive starvation response. Proceedings of the National Academy of Sciences of the U S A 106(26):10853—10858.

[29] Sauve, M., Ban, K., Momen, A., Zhou, Y.-Q., Henkelman, R.M., Husain, M., et al., 2010. Genetic deletion or pharmacological inhibition of dipeptidyl peptidase-4 improves cardiovascular outcomes following myocardial infarction in mice. Diabetes 59(4):1063—1073.

[30] Mulvihill, E.E., Varin, E.M., Gladanac, B., Campbell, J.E., Ussher, J.R., Baggio, L.L., et al., 2017. Cellular sites and mechanisms linking reduction of dipeptidyl peptidase-4 activity to control of incretin hormone action and glucose homeostasis. Cell Metabolism 25(1):152—165.

[31] Bainbridge, T.W., Dunshee, D.R., Kljavin, N.M., Skelton, N.J., Sonoda, J., Ernst, J.A., 2017. Selective homogeneous assay for circulating endopeptidase fibroblast activation protein (FAP). Scientific Reports 7(1):12524.

[32] Dunshee, D.R., Bainbridge, T.W., Kljavin, N.M., Zavala-Solorio, J., Schroeder, A.C., Chan, R., et al., 2016. Fibroblast activation protein cleaves and inactivates fibroblast growth factor 21. Journal of Biological Chemistry 291(11):5986—5996.

[33] Zhen, E.Y., Jin, Z., Ackermann, B.L., Thomas, M.K., Gutierrez, J.A., 2016. Circulating FGF21 proteolytic processing mediated by fibroblast activation protein. Biochemical Journal 473(5):605—614.

[34] Cunningham, C.C., 2007. Talabostat. Expert Opinion on Investigational Drugs 16(9):1459—1465.

[35] Jansen, K., Heirbaut, L., Cheng, J.D., Joossens, J., Ryabtsova, O., Cos, P., et al., 2013. Selective inhibitors of fibroblast activation protein (FAP) with a (4-Quinolinoyl)-glycyl-2-cyanopyrrolidine scaffold. ACS Medicinal Chemistry Letters 4(5):491—496.

[36] Fadini, G.P., Albiero, M., Menegazzo, L., de Kreutzenberg, S.V., Avogaro, A., 2012. The increased dipeptidyl peptidase-4 activity is not counteracted by optimized glucose control in type 2 diabetes, but is lower in metformin-treated patients. Diabetes, Obesity and Metabolism 14(6):518—522.

[37] Samms, R.J., Lewis, J.E., Norton, L., Stephens, F.B., Gaffney, C.J., Butterfield, T., et al., 2017. FGF21 is an insulin-dependent postprandial hormone in adult humans. The Journal of Cinical Endocrinology and Metabolism 102(10):3806—3813.

[38] Wagner, L., Klemann, C., Stephan, M., von Horsten, S., 2016. Unravelling the immunological roles of dipeptidyl peptidase 4 (DPP4) activity and/or structure homologue (DASH) proteins. Clinical and Experimental Immunology 184(3):265—283.

[39] Ghersi, G., Zhao, Q., Salamone, M., Yeh, Y., Zucker, S., Chen, W.T., 2006. The protease complex consisting of dipeptidyl peptidase IV and seprase plays a role in the migration and invasion of human endothelial cells in collagenous matrices. Cancer Research 66(9):4652—4661.

[40] Nygaard, E.B., Moller, C.L., Kievit, P., Grove, K.L., Andersen, B., 2014. Increased fibroblast growth factor 21 expression in high-fat diet-sensitive non-human primates (Macaca mulatta). International Journal of Obesity (Lond) 38(2):183—191.

[41] Badman, M.K., Pissios, P., Kennedy, A.R., Koukos, G., Flier, J.S., Maratos-Flier, E., 2007. Hepatic fibroblast growth factor 21 is regulated by PPARalpha and is a key mediator of hepatic lipid metabolism in ketotic states. Cell Metabolism 5(6):426—437.

[42] Singhal, G., Fisher, F.M., Chee, M.J., Tan, T.G., El Ouaamari, A., Adams, A.C., et al., 2016. Fibroblast growth factor 21 (FGF21) protects against high fat diet induced inflammation and islet hyperplasia in pancreas. PloS One 11(2) e0148252.

[43] Zeng, K., Tian, L., Patel, R., Shao, W., Song, Z., Liu, L., et al., 2017. Diet polyphenol curcumin stimulates hepatic Fgf21 production and restores its sensitivity in high-fat-diet-fed male mice. Endocrinology 158(2):277—292.

[44] Niedermeyer, J., Kriz, M., Hilberg, F., Garin-Chesa, P., Bamberger, U., Lenter, M.C., et al., 2000. Targeted disruption of mouse fibroblast activation protein. Molecular and Cellular Biology 20(3):1089—1094.

[45] Lo, A., Li, C.P., Buza, E.L., Blomberg, R., Govindaraju, P., Avery, D., et al., 2017. Fibroblast activation protein augments progression and metastasis of pancreatic ductal adenocarcinoma. JCI Insight 2(19).

Supplementary Figures

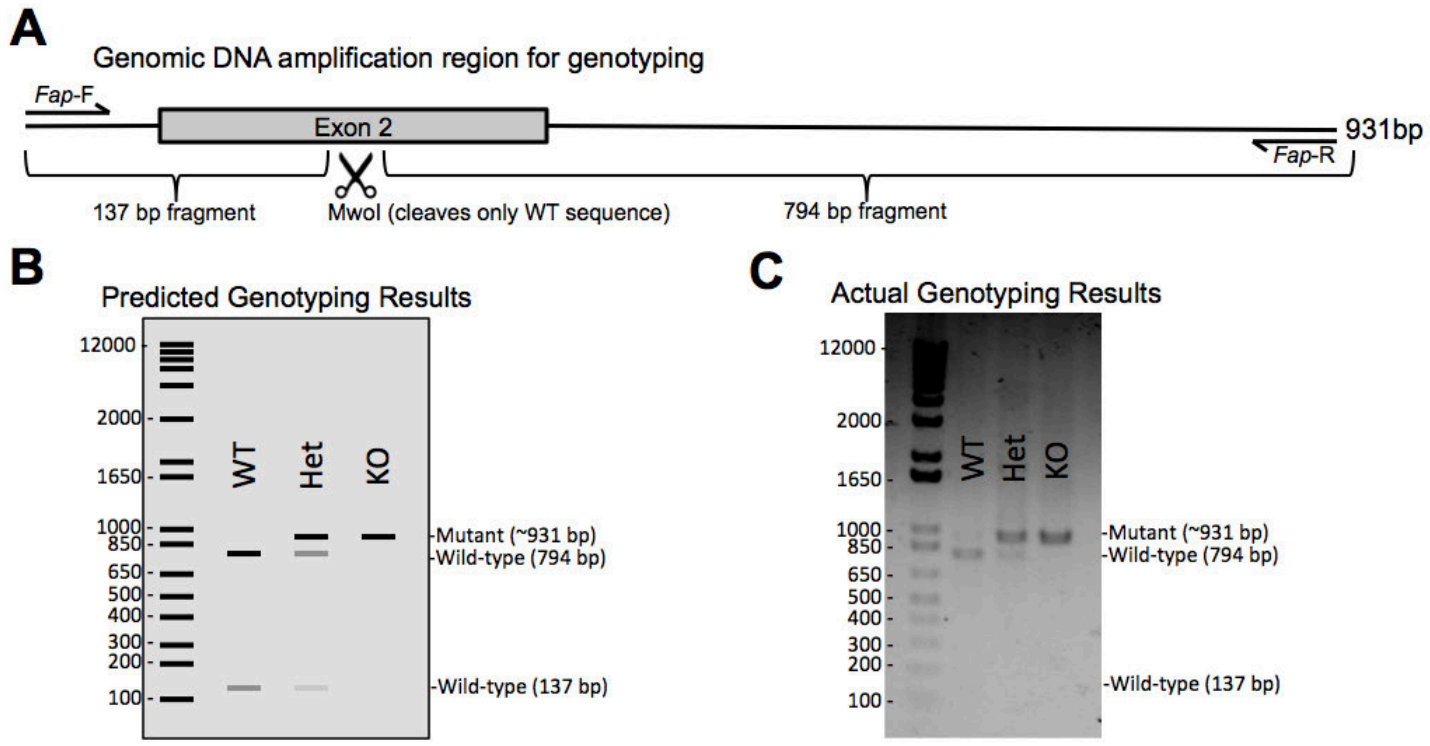

Figure S1: Genotyping of *Fap*$^{-/-}$ mouse lines using restriction enzyme digestion. Genotyping primers were designed to flank Exon 2, including targeted CRISPR/Cas9 mutagenesis site, to amplify a 931bp segment of genomic DNA. After PCR amplification, the product is subjected to digestion by Mwo1, which results in near complete digestion of wild-type (WT) PCR product. Partial digestion occurs for heterozygous (Het) samples, and no digestion occurs for knockout (KO) samples. **A)** Primer map of genomic DNA fragment, including Exon 2, Mwo1 cleavage site, and predicted fragment sizes. **B)** Predicted genotyping results and band sizes. **C)** Actual genotyping results for all genotypes.

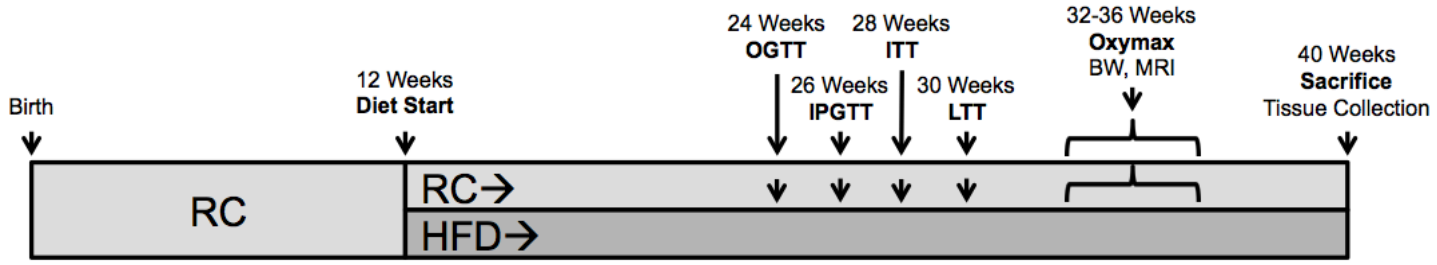

Figure S2: Chronic RC and HFD experimental timeline. All mice are raised on rodent chow (RC) and then at 12 weeks of age are assigned to continue on RC or be switched to 45% high-fat diet (HFD). Beginning at 24 weeks, mice are subjected to oral glucose tolerance test (OGTT), intraperitoneal glucose tolerance test (IPGTT), insulin tolerance test (ITT), lipid tolerance test (LTT) in 2 week intervals. Between 32-36 weeks of age, the mice have body-composition measurements, and are then placed in individual Oxymax chambers in random order for indirect calorimetry and food intake measurements. At 40 weeks of age, the mice are sacrificed and tissues collected for protein and mRNA analyses. In HFD-fed mice, body-weights (BW) are measured periodically, including on test days, to monitor weight gain over time.

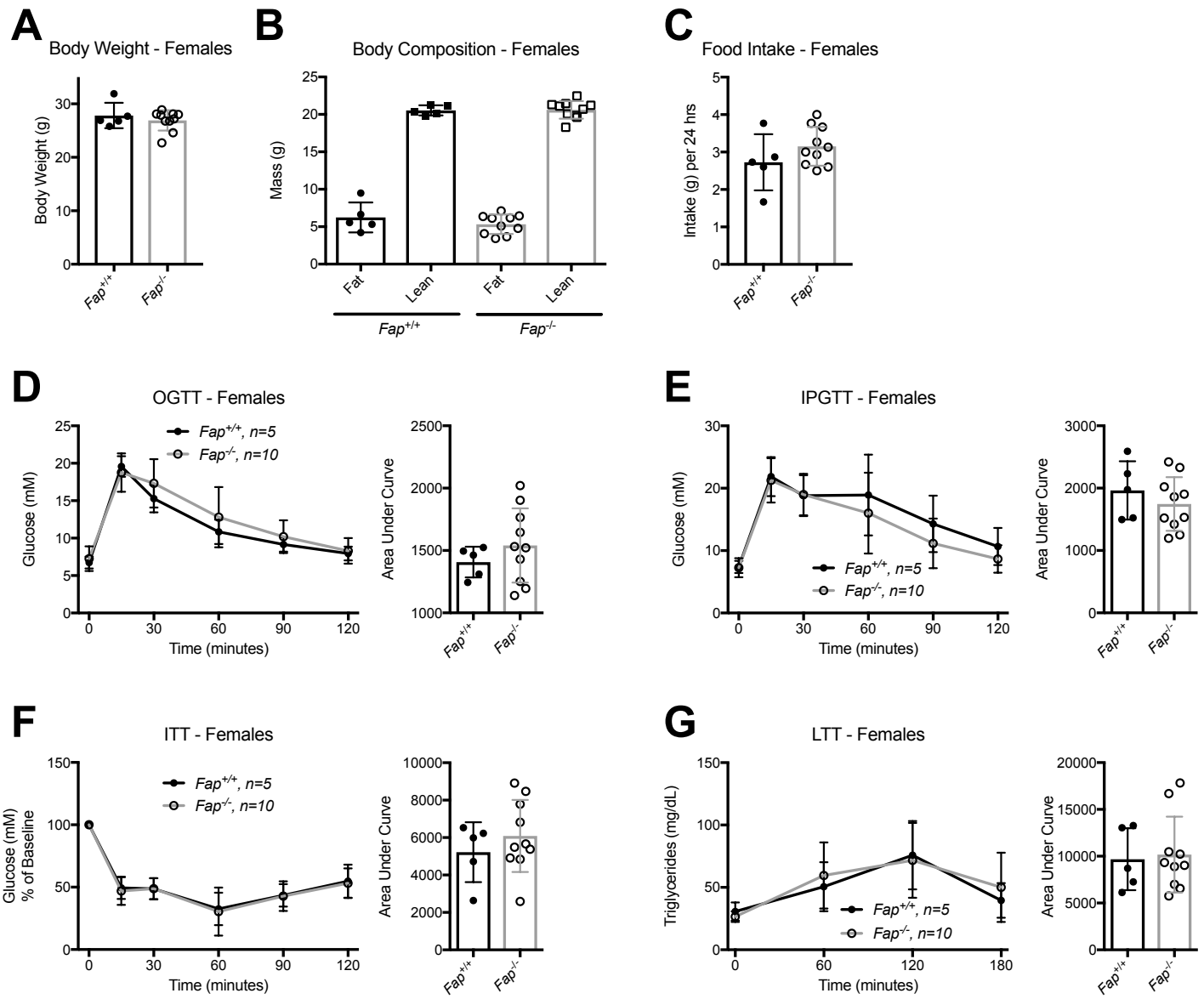

Figure S3: Female *Fap*$^{-/-}$ mice fed normal rodent chow exhibit normal glucose and lipid tolerance. Female mice were subjected to the same treatment as RC-fed male mice (Figure S3) and studied simultaneously. **A)** Body weight. **B)** Body composition. **C)** Food intake. **D)** OGTT and AUC analysis. **E)** IPGTT and AUC analysis. **F)** ITT and AUC analysis. **G)** TGs during LTT and AUC analysis. AUC data was further analyzed using two-tailed *t*-test.

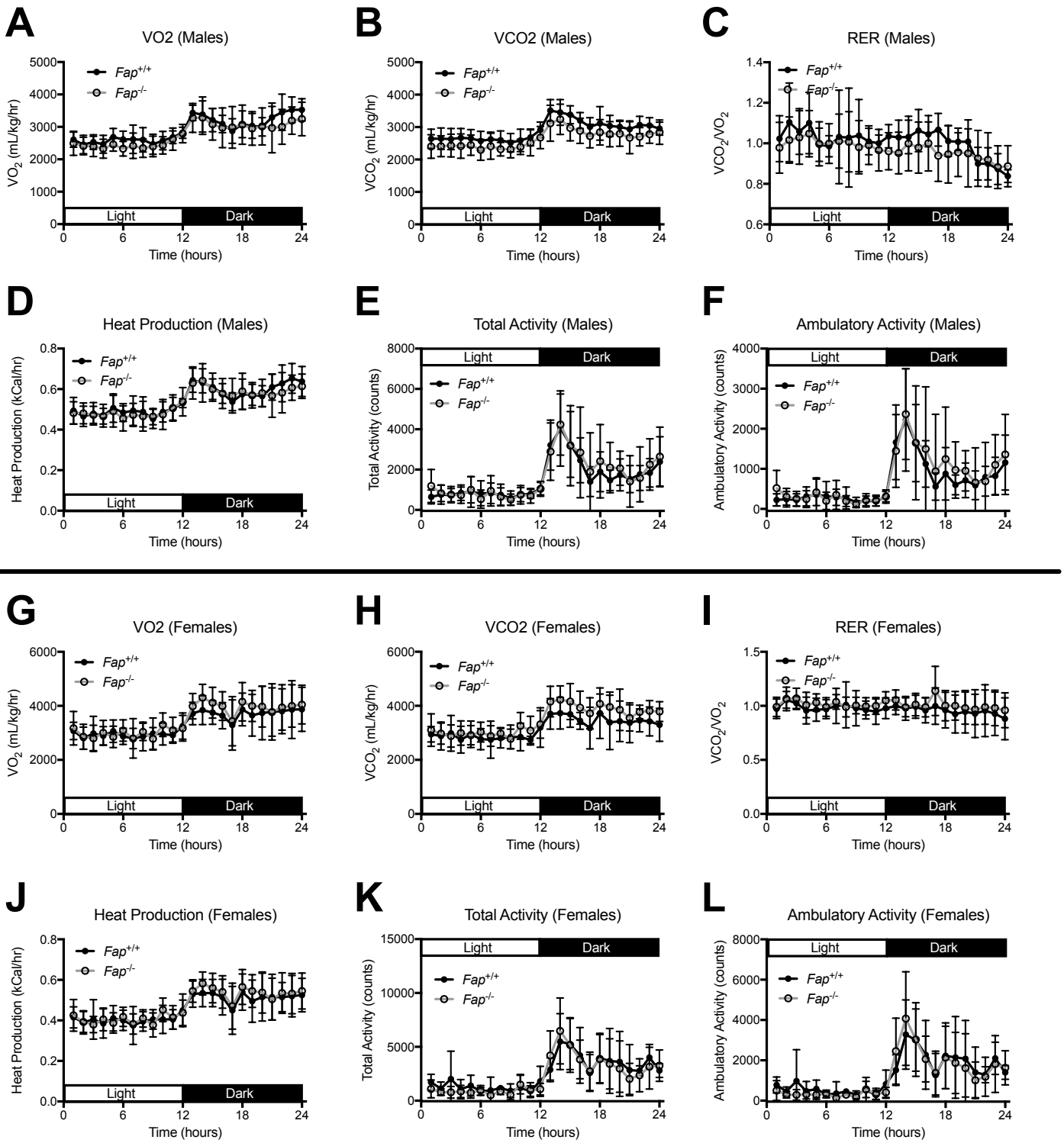

Figure S4: Parameters of energy expenditure are similar in *Fap*$^{-/-}$ vs. *Fap*$^{+/+}$ mice on a RC diet. Adult male and female Fap+/+ and -/- mice underwent indirect calorimetry measurement of several metabolic parameters. **A-F)** Measurements of VO_2, VCO_2, RER, Heat Production, Total Activity, and Ambulatory Activity in male mice. **G-L)** Corresponding measurements of VO_2, VCO_2, RER, Heat Production, Total Activity, and Ambulatory Activity in female mice. Because there were no differences in body weight or body composition, all expenditure values are normalized to body weight.

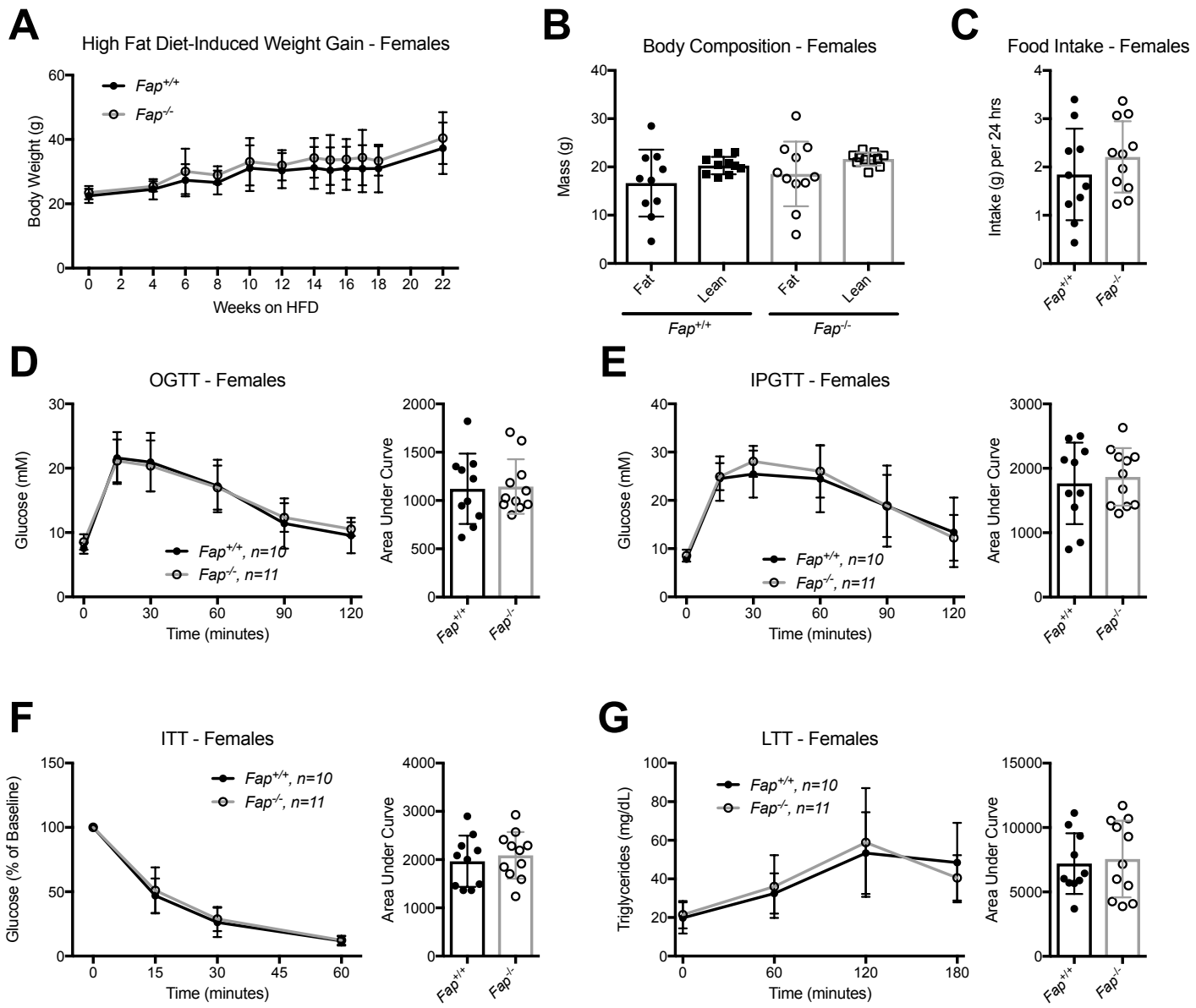

Figure S5: Female *Fap*$^{-/-}$ mice fed chronic high-fat diet exhibit no metabolic defects. Female mice were subjected to the same treatment as the RC-fed male mice Figure S3) and studied simultaneously. **A)** Body weight. **B)** Body composition. **C)** Food intake. **D)** OGTT and AUC analysis. **E)** IPGTT and AUC analysis. **F)** ITT and AUC analysis. **G)** TGs during LTT and AUC analysis. AUC data was analyzed using two-tailed *t*-test.

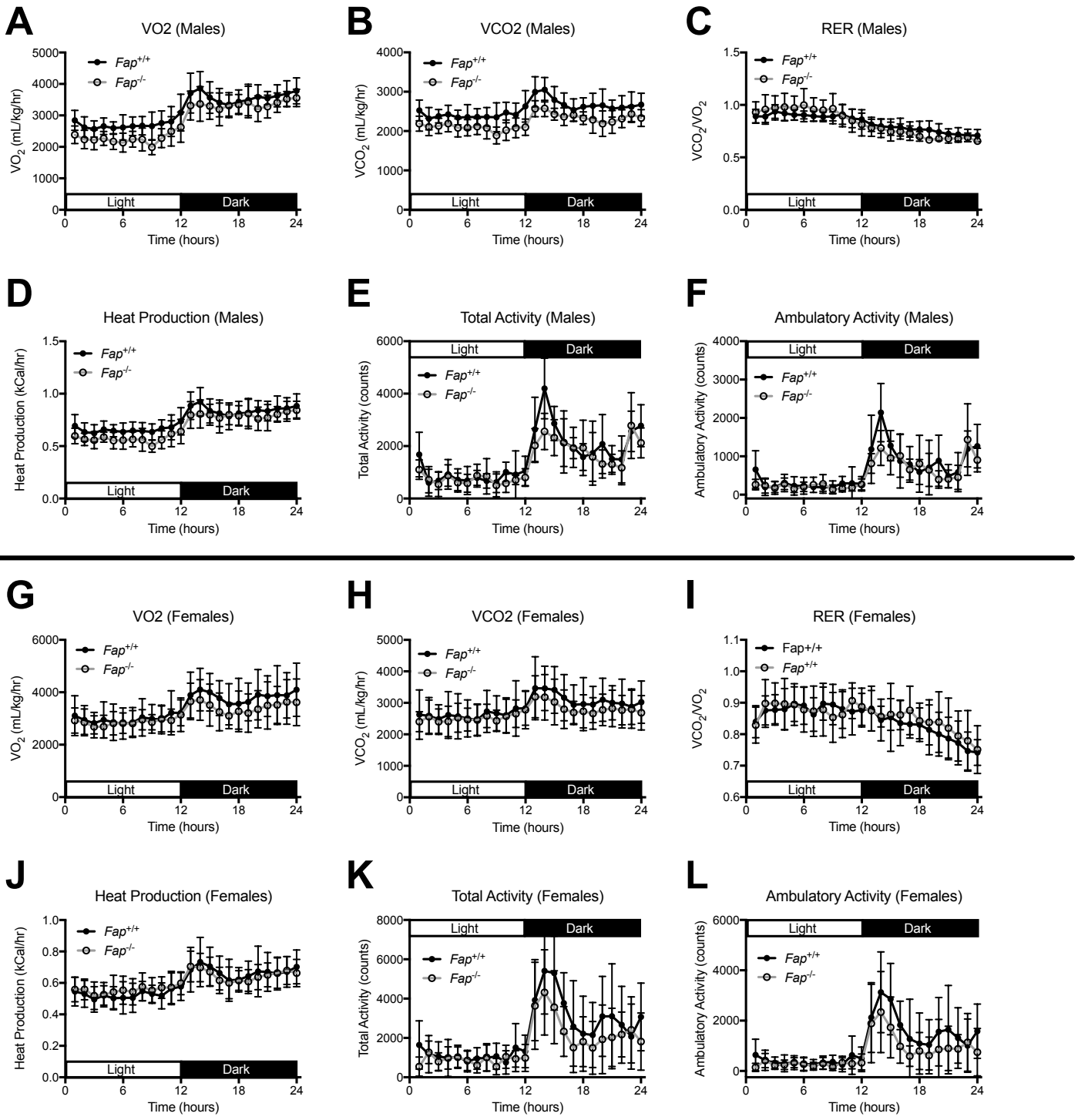

Figure S6: *Fap*$^{-/-}$ mice are metabolically similar to *Fap*$^{+/+}$ mice when fed a normal RC diet. Adult male and female *Fap*$^{+/+}$ and $^{-/-}$ mice underwent indirect calorimetric measurement of several metabolic parameters. **A-F)** Measurements of VO_2, VCO_2, RER, Heat Production, Total Activity, and Ambulatory Activity in male mice. **G-L)** Corresponding measurements of VO_2, VCO_2, RER, Heat Production, Total Activity, and Ambulatory Activity in female mice. Because there were no differences in body weight or body composition, all expenditure values are normalized to body weight.

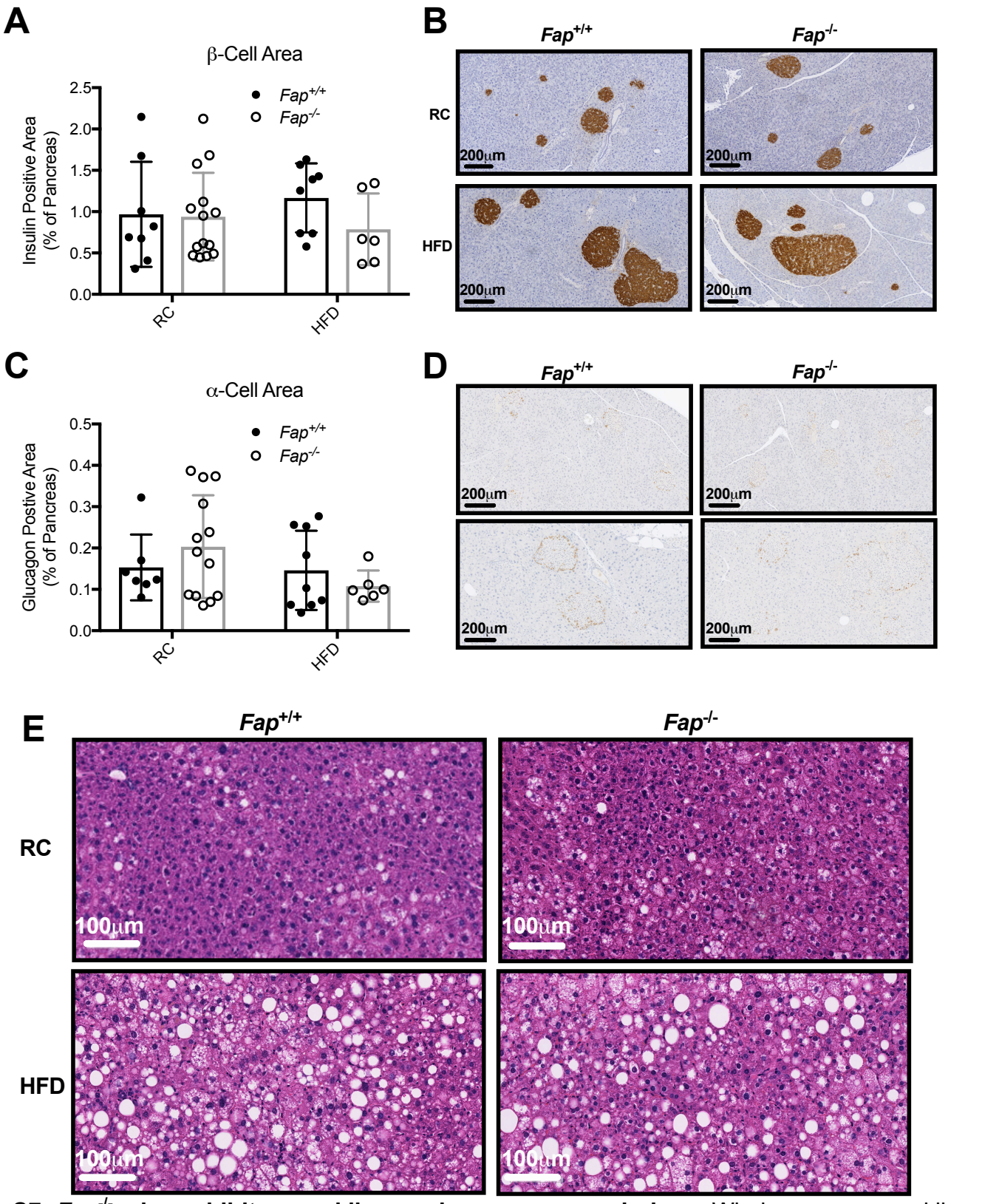

Figure S7: *Fap*$^{-/-}$ mice exhibit normal liver and pancreas morphology. Whole pancreas and liver was removed from 40-week old male *Fap*$^{+/+}$ and *Fap*$^{-/-}$ fed either chronic RC of HFD. Sections mounted on slides for either insulin or glucagon (pancreas) or H&E stained (liver). **A)** β-Cell area (insulin-positive area) or **B)** Representative insulin-stained sections from each experimental condition. **C)** α-Cell area (glucagon-positive area). **D)** Representative glucagon-stained sections from each condition. **E)** Representative H&E-stained liver images from each experimental condition. No statistical significance was detected using 2-way ANOVA.

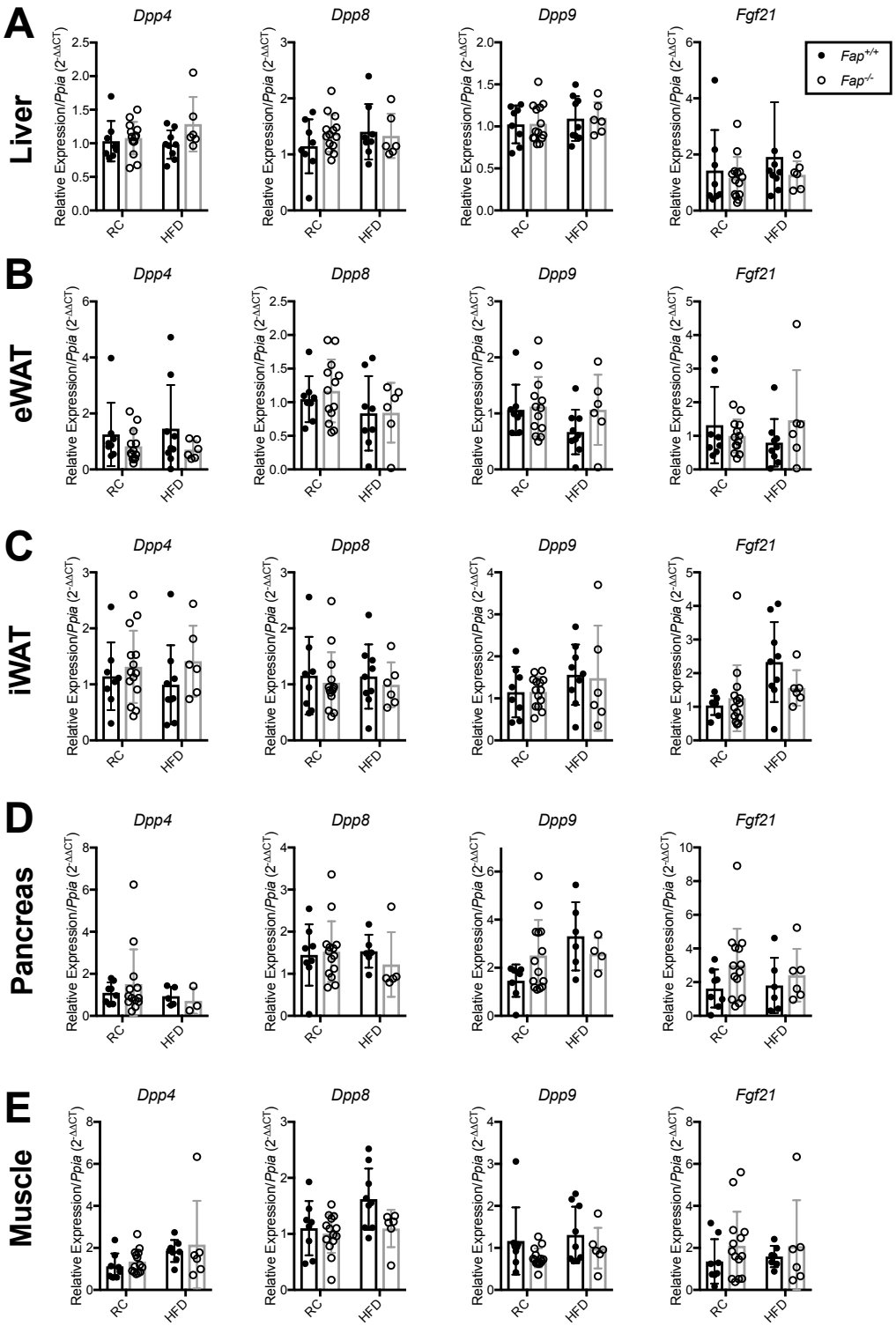

Figure S8: ***Gene expression analysis of DASH family and*** **Fgf21** ***mRNA transcripts*** Tissues were collected from 40-week old male *Fap*$^{+/+}$ and *Fap*$^{-/-}$ mice following chronic RC or HFD feeding. Expression levels of *Dpp4*, *Dpp8*, *Dpp9*, and *Fgf21* mRNA were measured in the listed tissues and expressed relative to levels of endogenous control mRNA, *Ppia,* and normalized to *Fap*$^{+/+}$ RC animals ($2^{-\Delta\Delta CT}$). **A)** Liver. **B)** Epididymal white adipose tissue (eWAT). **C)** Inguinal white adipose tissue (iWAT). **D)** Pancreas. **E)** Muscle. All data were analyzed using 2-way ANOVA and no significant differences were found.

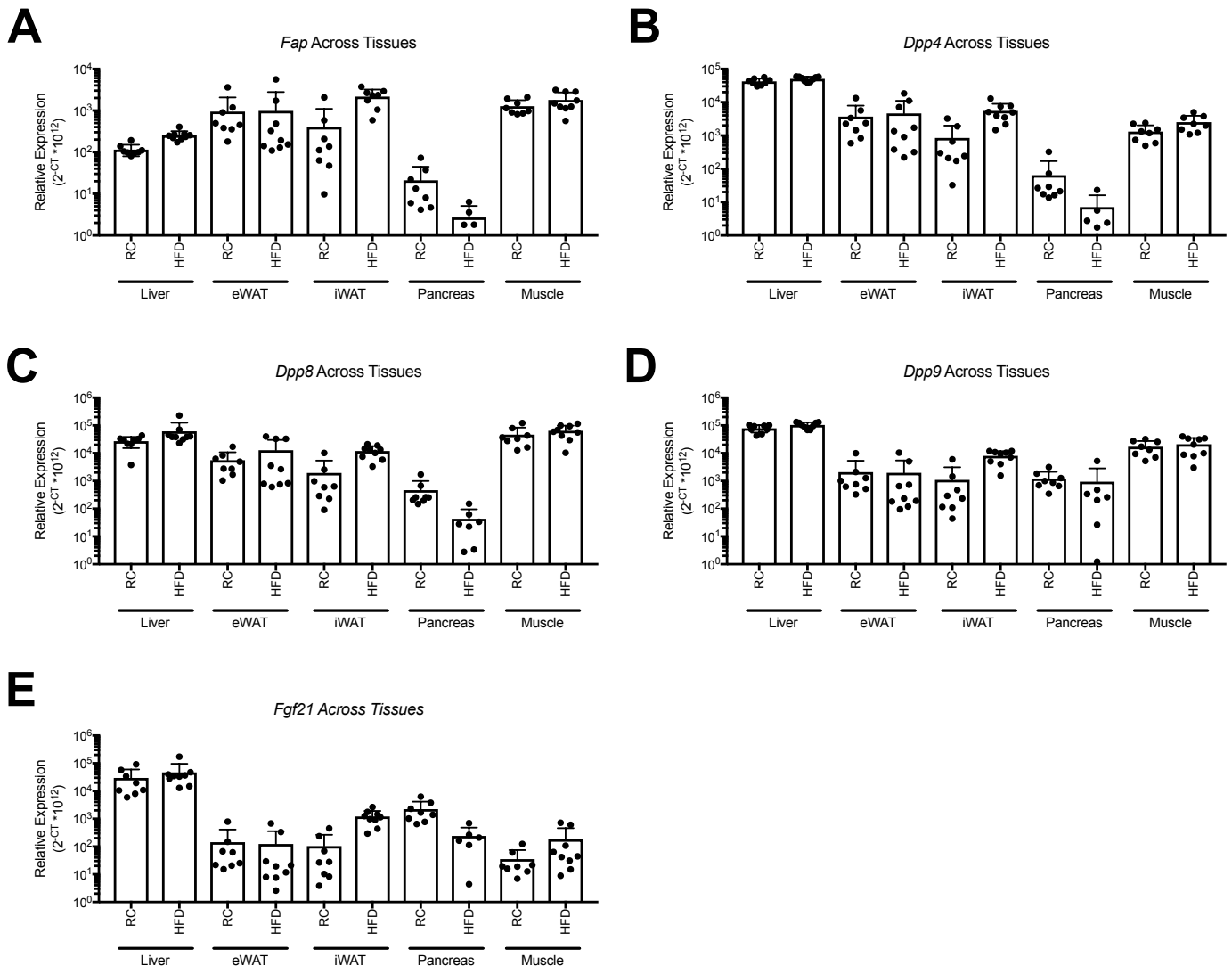

Figure S9: Relative tissue expression profiles of *Fap*, *Dpp4*, *Dpp8*, *Dpp9*, and *Fgf21*. Tissues were collected from 40-week old male $Fap^{+/+}$ mice following chronic RC or HFD feeding. Expression levels of *Fap*, *Dpp4*, *Dpp8*, *Dpp9*, and *Fgf21* mRNA were measured in the listed tissues and expressed as $2^{-CT}X10^{12}$ to estimate relative expression levels of each gene across liver, epididymal white adipose tissue (eWAT), inguinal white adipose tissue (iWAT), pancreas, and muscle. **A)** *Fap* expression across tissues. **B)** *Dpp4* expression across tissues. **C)** *Dpp8* expression across tissues. **D)** *Dpp9* expression across tissues. **E)** *Fgf21* expression across tissues.